Optical Characterization of Silicon Nitride-based Bilayer Thin Films Using Spectroscopic Ellipsometry and the Maxwell-Garnett Model

Abdelaziz Beddiaf[1,3,*], Malika Medjaldi[1], Djemouai Djamai[2], Abderrahim Lanani[1]
[1]*SATIT Laboratory, Abbes Laghrour University, Khenchela, Algeria*
[2]*Laboratory of Engineering and Sciences of Advanced Materials (ISMA), Abbes Laghrour University, Khenchela, Algeria*
[3]*MoDERNa Laboratory, University of Constantine 1, Route d' Ain El Bey, 25000 Constantine, Algeria*
[*]*beddiafaziz@univ-khenchela.dz; malika.medjaldi@univ-khenchela.dz; djamai_djmouai@univ-khenchela.dz; lanani_arahim@univ-khenchela.dz*

***Abstract*—This study investigates the optical and geometrical properties of silicon oxynitride (SiO_xN_y) thin films, which were prepared using a low-pressure chemical vapor deposition (LPCVD) process at 850 °C from SiH_2Cl_2, N_2O, and NH_3 as precursors. The opto-geometrical parameters of these were determined through spectroscopic ellipsometry measurements, employing the Maxwell-Garnett model for data analysis. This model posits silicon oxynitride as a heterogeneous medium composed of silicon oxide (SiO_2) and silicon nitride (Si_3N_4). The refractive index of SiO_xN_y was computed as a function of both wavelength and gas flow ratio NH_3/N_2O, and was further evaluated based on the volume fraction of its constituents and film thickness. Subsequently, the effect of deposition time on film thickness and refractive index was examined. It was observed that the refractive index decreases with increasing wavelength, yet increases with both the gas flow ratio and film thickness, ranging from 1.457 to 1.618. The results also indicate that the SiO_2 volume fraction decreases as the NH_3/N_2O ratio increases, while the Si_3N_4 volume fraction concurrently increases. They equally indicate that prolonged deposition time leads to a significant increase in film thickness and a higher refractive index. This study provides a fundamental basis for selecting deposition parameters that are tailored to specific applications.**

***Index Terms*—Ellipsometry; Silicon oxynitride; Refractive index; Maxwell-Garnett.**

I. INTRODUCTION

Silicon dioxide (SiO_2), with a refractive index of 1.46, exhibits a good transparency in the visible range, excellent dielectric properties (Eg~10eV), and low mechanical stress. However, it functions as a poor barrier against the diffusion of ions and dopants [1]–[5]. In contrast, silicon nitride Si_3N_4, which has a refractive index of 2.02, is denser and therefore provides a more effective diffusion barrier. Nevertheless, it is a mediocre dielectric (Eg~5.5eV) and has low crack resistance due to significant mechanical stress [6]–[10]. To mitigate these limitations, it has become appealing to find a compromise between the properties of these two silicon-based compounds by fabricating intermediate materials [2], [3].

Silicon oxynitride (SiO_xN_y) combines the dielectric and mechanical qualities of silica, along with the advantage of serving as a diffusion barrier to impurities, distinguished by the nitrides. It is a promising candidate for the production of antireflective coatings and is also used in waveguides, integrated optics, and microelectronics, as intermetallic insulators and passivation insulators [11]–[15].

The comprehensive study of the characteristics of these materials is crucial to defining their optical, physical, and chemical properties. Accordingly, numerous studies have been conducted in this field. For instance, research by Makasheva [16] focuses on analyzing the structural, physico-chemical, and electrical characteristics of the silicon nitride-oxide layers deposited as either single or multilayer structures. Her approach is based on the ability to assemble structures with graded properties and control the conductive properties of the multilayer system during deposition. Subsequently, Mahamdi *et al.* [17] presented the properties of thin SiO_xN_y films fabricated using the plasma-enhanced chemical vapor deposition (PECVD) technique from a mixture of silane SiH_4, nitrous oxide (N_2O), ammonia (NH_3), and nitrogen (N_2). The same authors have indicated the effect of the gas mixture $SiH_4/N_2O/NH_3/N_2$ on the properties of SiO_xN_y thin layers realized by PECVD [18]. Then, the study of the charging effect of a-SiO_xN_y:H thin films using Kelvin force microscopy to determine the local electrical parameters of the films is the subject of the research work of Villeneuve-Faure [19]. Recently, Boulesbaa [20] have analyzed the vibrational properties of amorphous SiO_xN_y:H thin layers deposited on a silicon substrate using the PECVD processes. More recently, Yang *et al.* [21] have investigated the growth mechanism of SiO_xN_y films realized via plasma enhanced atomic layer deposition at low temperatures (100 °C–300 °C) using a tetraisocyanate silane ($Si(NCO)_4$) precursor and N_2 plasma.

Manuscript received 30 August, 2025; accepted 20 October, 2025.

This paper aims to study the opto-geometric properties of silicon oxynitride. For this purpose, different samples were elaborated using the low-pressure chemical vapor deposition (LPCVD) technique using SiH_2Cl_2, N_2O, and NH_3 gaseous precursors. The spectroscopic ellipsometry spectra were fitted using the Maxwell-Garnett (MG) model. This effective medium theory estimates the effective dielectric properties of a composite material considering the volume fractions and properties of its constituents [22]–[26]. In this case, the model was applied by assuming the silicon oxynitride material as a heterogeneous medium, composed of silicon oxide (SiO_2) and silicon nitride (Si_3N_4) [2], [22].

II. Experimental Process

Thin layers of silicon oxynitride were deposited on a single-crystal silicon substrate using the LPCVD technique, with a mixture of dichlorosilane (SiH_2Cl_2), nitrous oxide (N_2O), and ammonia (NH_3) as precursors. The flow rates of SiH_2Cl_2 and the combination [$N_2O + NH_3$] were kept constant, respectively, at 200 and 160 sccm throughout the deposition process, while the gas flow ratio [NH_3/N_2O] varied from 0.03 to 0.23. The sample series was deposited at a temperature of 850 °C and a pressure of 450 mTorr for 50 minutes.

Spectroscopic ellipsometry measurements of the fabricated films were carried out using a rotating analyzer ellipsometer, model SpecEL2000-VIA. These measurements correspond to the ellipsometric angles Ψ and Δ, which were independently extracted as a function of wavelength over a measurement range from 450 nm to 900 nm, with an incidence angle of 70 °, as shown in Fig. 1.

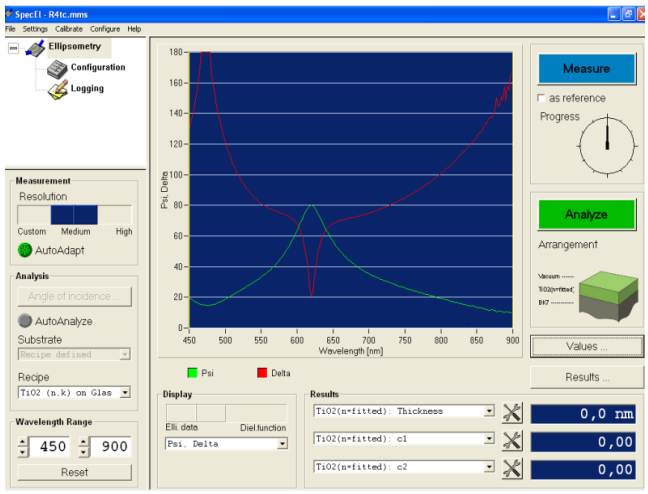

Fig. 1. User space of spectroscopic ellipsometry (sample, where R = 0.14).

To determine the refractive index and thickness of the layers studied, these measured angles will be superimposed and compared with those calculated by the proposed model through a fitting procedure.

III. Modeling and Governing Equation

In this study, we use the ellipsometric method, which is defined by the ratio of complex Fresnel reflection coefficients and is based on the fundamental equation presented in [23]–[25]

$$\rho = \frac{R_p}{R_S} = \tan\psi e^{j\Delta}. \tag{1}$$

In this equation, Ψ and Δ represent the ellipsometric angles in degrees.

The refractive index of the mixture, obtained by using the Maxwell-Garnett model, is expressed in (2). This model is better suited for nanocomposites and optical materials than the Bruggeman effective medium approximation [26], [27]

$$\frac{n^2_{SiO_xN_y} - n^2_{SiO_2}}{n^2_{SiO_xN_y} + 2n^2_{SiO_2}} = \left(1 - f_{SiO_2}\right)\frac{n^2_{Si_3N_4} - n^2_{SiO_2}}{n^2_{Si_3N_4} + 2n^2_{SiO_2}}. \tag{2}$$

This equation can be simplified as follows

$$\left(n^2_{Si_3N_4} + 2n^2_{SiO_2} + f_{SiO_2}\left(n^2_{SiO_2} - n^2_{Si_3N_4}\right)\right)n^2_{SiO_xN_y} - \\ -(2f_{SiO_2} + 1)n^2_{SiO_2}n^2_{Si_3N_4} - (2 - 2f_{SiO_2})n^4_{SiO_2} = 0, \tag{3}$$

with

$$f_{SiO_2} + f_{Si_3N_4} = 1. \tag{4}$$

where $n_{SiO_xN_y}$ is the refractive index of the studied films, while f_{SiO_2} and $f_{Si_3N_4}$ represent the volume fractions of the SiO_2 and Si_3N_4, respectively. The refractive indices n_{SiO_2} and $n_{Si_3N_4}$ were taken from the work in [28].

A simplex method was employed to minimize the error function (5) [2], allowing us to overlay the theoretical curves of the angles ψ^i_{th} and Δ^i_{th} calculated by our model with the experimental data (ψ^i_{exp} and Δ^i_{exp}). This was achieved by adjusting the values of the thickness and volume fraction of one of the two constituents

$$\chi^2 = \frac{1}{N}\sum_{i=1}^{N}(\psi^i_{\text{exp}} - \psi^i_{th})^2 + (\Delta^i_{\text{exp}} - \Delta^i_{th})^2. \tag{5}$$

In this context, *N* represents the number of measurements. Since Ψ and Δ are in degrees, the error metric χ^2 is expressed in degrees squared.

IV. Results and Discussion

A. The Maxwell-Garnett Model Validation

To validate the Maxwell-Garnett model, we compared the results obtained from the model with those established experimentally. In the LPCVD process, gas flow rates are regulated using calibrated mass flow controllers (MFCs), which report flow rates in standard cubic centimeters per minute (sccm). For this study, we focused on the sample deposited with an ammonia flow rate of 20 sccm and a nitrous oxide flow rate of 140 sccm.

Using the minimization procedure, the theoretical curves were successfully fitted to the experimental data, resulting in an error of 3.16×10^{-6}. The calculated error metric,

corresponding to the mean squared deviation between experimental and theoretical ellipsometric angles, aligns with results reported in previous ellipsometric modeling studies [17], [20]. This demonstrates a high degree of accuracy in fitting the theoretical curves to the experimental spectra, as shown in Figs. 2(a) and 2(b). These results confirm that the minimization technique in the proposed model aligns with the experimental findings, demonstrating the model's effectiveness.

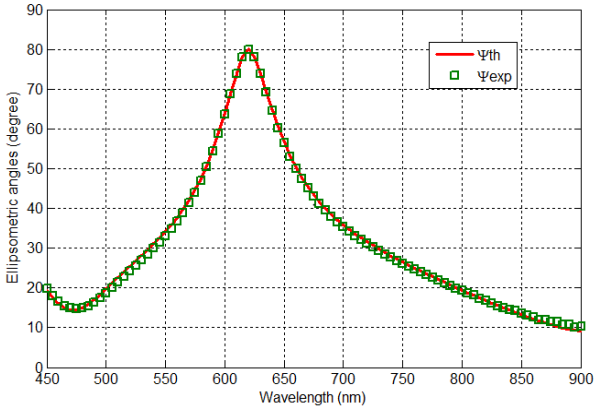

(a)

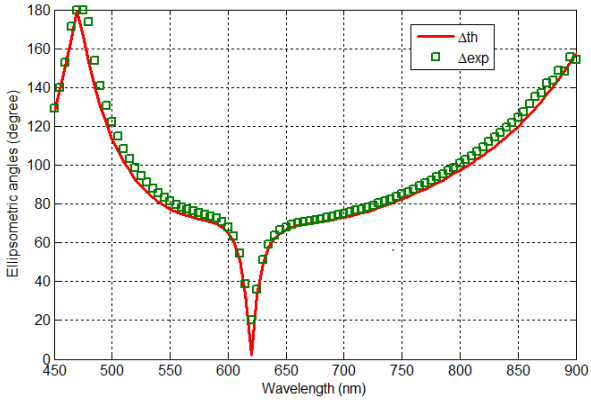

(b)

Fig. 2. Experimental and calculated spectra of the ellipsometric angles for an oxynitride layer obtained with R = 0.14 and t = 50 min: (a) Ψ; (b) Δ.

B. *Optical and Geometrical Parameters*

In this section, the variation of the refractive index of SiO_xN_y has been performed for numerous parameters, such as wavelength, volume fraction, gas flux ratio, and thickness, using Figs. 3 to 7. Based on the results shown in Fig. 3, we can see that the profile of refractive index of SiO_xN_y is a decreasing function with wavelength. Nevertheless, at wavelength $\lambda = 830$ nm, where the extinction coefficient was zero, the refractive index increases from that of SiO_2 to that of Si_3N_4 as the gas flux ratio $R = NH_3/N_2O$ increases (Fig. 4), ranging from 1.457 to 1.618. This can be attributed to the gradual increase in the incorporation of the NH_3 flow rate into the SiO_xN_y films.

At a wavelength of 830 nm, the silicon oxynitride films exhibit high transparency and behave as a non-absorbing medium; this improves the accuracy of refractive index determination by minimizing absorption effects. To further examine the effect of the constituent volume fractions, such as the percentages of SiO_2 and Si_3N_4, on the refractive index of SiO_xN_y at this wavelength, we plot their variations in Figs. 5 and 6. Figure 5 shows that the refractive index is inversely proportional to the volume fraction of SiO_2, which can be explained by the decrease in the gas flow that controls oxygen (N_2O). Conversely, the refractive index is proportional to the percentage of Si_3N_4, as indicated in Fig. 6. This proportionality is justified by the elevation in the flow rate of ammonia gas, which governs the nitrogen content, which is logical.

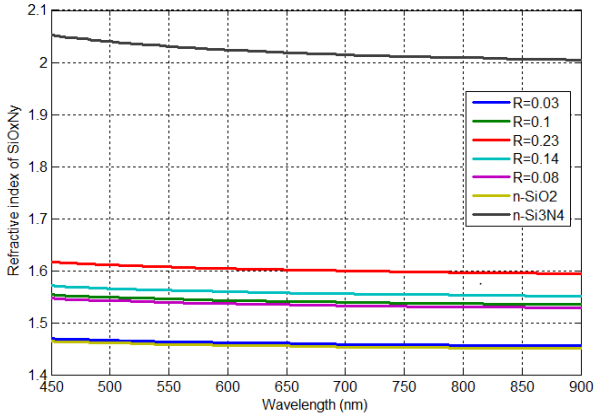

Fig. 3. Evolution of the refractive index versus wavelength.

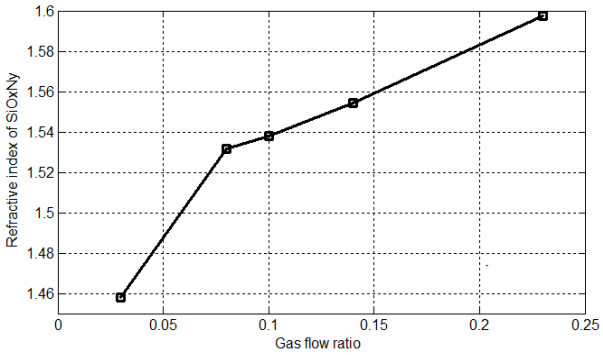

Fig. 4. Refractive index as a function of the gas flow ratio $R = NH_3/N_2O$ at 830 nm.

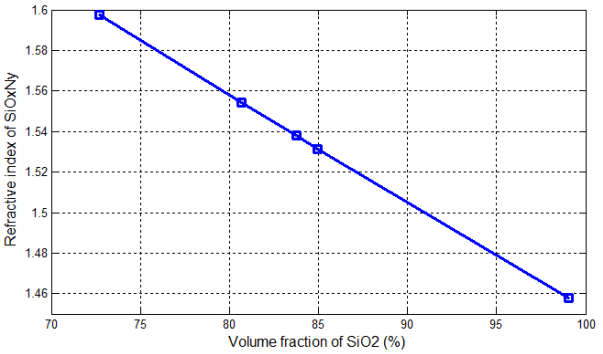

Fig. 5. Variation of the refractive index versus volume fraction of SiO_2 at 830 nm.

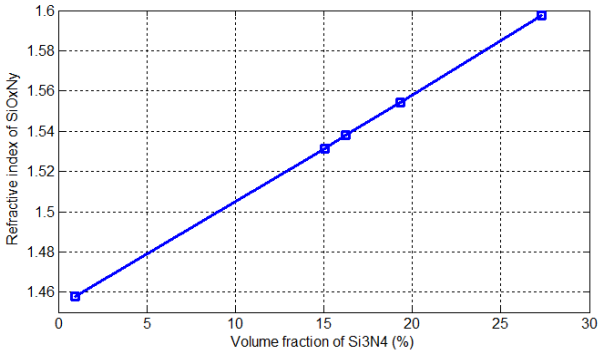

Fig. 6. Variation of the refractive index versus the volume fraction of Si_3N_4 at 830 nm.

The silicon oxynitride (SiO_xN_y) film with a volume fraction 1 % of silicon nitride Si_3N_4 (Fig. 6), behaves almost like silicon dioxide SiO_2, making it a suboptimal choice in terms of optical properties. Therefore, to achieve good optical characteristics for this material, its refractive index must remain between those of its constituents.

To highlight the evolution of the optical properties of the elaborated films at the same wavelength (λ = 830 nm), the refractive index is analyzed by varying several thickness values. From Fig. 7, we observe that the refractive index is an increasing function as the thickness changes between 287 nm and 398 nm. The increase in film thickness is attributed to the higher ammonia flow rate. The introduction of larger quantities of reactive gases, specifically ammonia and nitrous oxide, leads to a progressive thickening of the silicon oxynitride films. These films are suitable for application in nanoscale devices [3], [20].

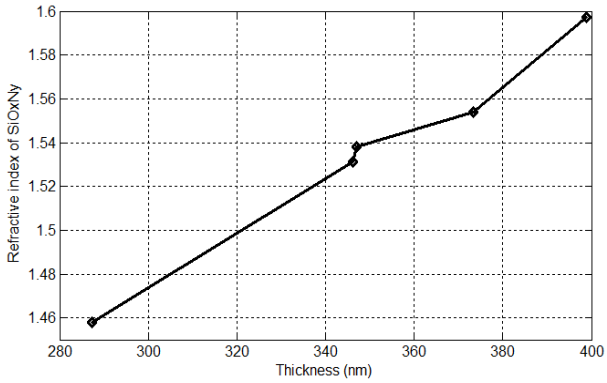

Fig. 7. Refractive index variation vs. thickness films at λ = 830.

As previously mentioned, the main part of this study is devoted to the optical properties of the SiO_xN_y films. The percentage of SiO_2 and that of Si_3N_4 define the values of its refractive index. Knowledge of their variations with gas flow ratio is used to quantify the evolution in the refractive index of SiO_xN_y. According to Fig. 8, it can be noticed that the volume fraction of SiO_2 continues to decrease as the ratio R is increases. In this case, the highest value of the silica percentage (99 %) is obtained for an oxynitride film with a thickness of 287 nm and a refractive index equal to 1.458. Moreover, the volume fraction of Si_3N_4 increases with the gas flow ratio. As a result, the refractive index of SiO_xN_y is increasingly approaching that of Si_3N_4.

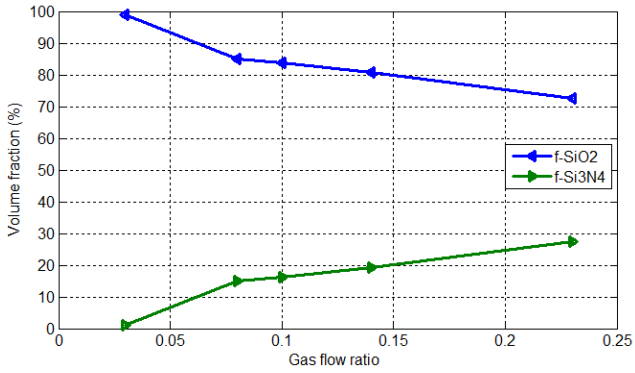

Fig. 8. Volume fraction of SiO_2 and of Si_3N_4 variation with gas flow ratio.

On the other hand, this study also allows for the investigation of the impact of the deposition time of the films on the thickness, as well as on the refractive index of these thin layers. To achieve this, two samples were prepared under the same experimental deposition parameters, with a gas flow ratio of R = 0.08 for two different deposition times.

Before proceeding to the analysis of the obtained results, we first show in Fig. 9 the strong agreement between the experimental and theoretical profiles of the ellipsometric angles of the film deposited during a time t = 160 min. This deposition resulted in significant growth of the SiO_xN_y film thickness, reaching 1066 nm. In contrast, the thickness of the film deposited with the same gas flow ratio but for a shorter time period (t = 50 min) is 346 nm. The prolonged deposition time allows the introduction of more reactive gases. So, the amount of nitrous oxide that governs the oxygen and the ammonia controlling the nitrogen multiply, resulting in a very thick silicon oxynitride film, which is a drawback.

Additionally, in Fig. 10, we present the refractive index profiles of these two samples. We observe that the refractive index is higher for the layer developed during t = 160 min, due to the significant influence of the deposition time on the incorporation of the silicon nitride phase in the film. Therefore, to increase the refractive index, extending the deposition time is an effective approach. This option is easy to implement and does not affect their properties; however, it leads to an increase in film thickness. Consequently, a balance between thickness and refractive index should be considered.

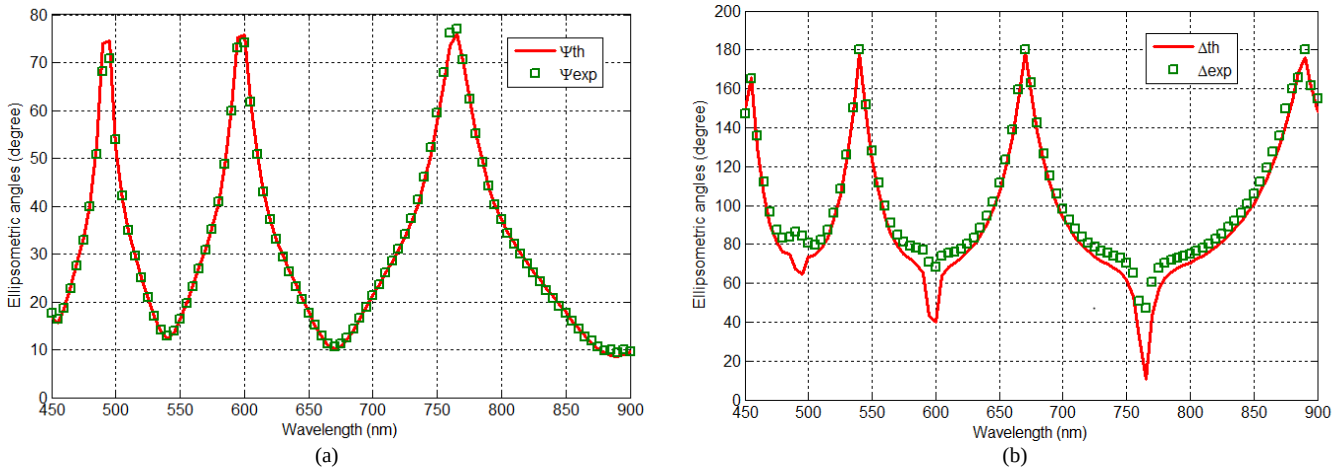

Fig. 9. Experimental and calculated spectra of the ellipsometric angles for oxynitride layers obtained with R = 0.08 and t = 160 min: (a) Ψ; (b) Δ.

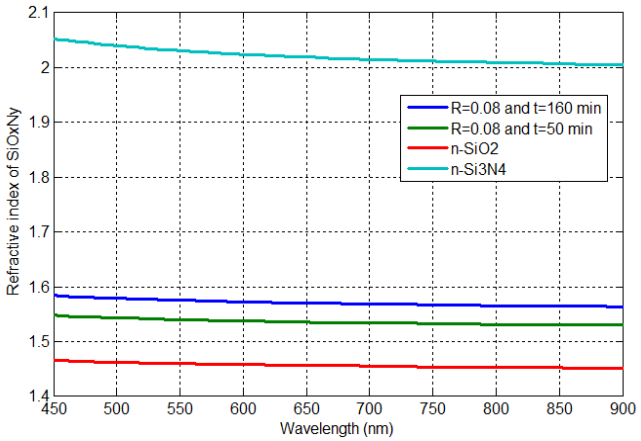

Fig. 10. Refractive index as a function of wavelength for R = 0.08 by changing the deposition time: t = 50 min and t = 160 min.

Table I summarizes the results obtained in this part by optimizing the error function (5) using the MG model.

TABLE I. THE ESTIMATED VALUES OF THICKNESS, VOLUME FRACTION, AND REFRACTIVE INDEX WERE OBTAINED BASED ON THE MG MODEL.

Gas flow ratio	Times (min)	Thickness (nm)	Percentage (%)		$n_{SiO_xN_y}$ at 830 nm
			f_{SiO_2}	$f_{Si_3N_4}$	
Samples S2 and S6: R = 0.08	50	346	84.94	15.06	1.531
	160	1066	78.52	11.48	1.566

V. CONCLUSIONS

In summary, this research paper contributes to the study of the opto-geometric parameters of silicon oxynitride SiO_xN_y, thin films prepared by the low-pressure chemical vapor deposition process (LPCVD), using spectroscopic ellipsometry data and the Maxwell-Garnett model. The comparison between the spectra obtained from the model and those collected experimentally validates the effectiveness of the model.

The results indicate that the refractive index of SiO_xN_y decreases with increasing wavelength. However, at wavelength $\lambda = 830$ nm, where the extinction coefficient is zero, the refractive index of the realized films varies from the refractive index of SiO_2 to that of Si_3N_4 as the gas flow ratio NH_3/N_2O increases. This can be justified by the progressive increase in the NH_3 incorporation rate in the films produced.

Furthermore, we attempted to study the influence of both the thickness and the volume fraction of its constituents on the refractive index. The results proved that the refractive index increases as the thickness varies from 287 nm to 398 nm. They also demonstrate that the evolution of the refractive index is inversely proportional to the percentage of SiO_2, which can be explained by the decrease in the gas flow rate of nitrous oxide (N_2O). In the contrary, it is directly proportional to the volume fraction of the Si_3N_4, likely due to the increase in the flow rate of ammonia gas (NH_3) controlled nitrogen. Additionally, the results showed that the variation of the volume fraction of SiO_2 and Si_3N_4 with the gas flow ratio allows for quantifying the evolution of the refractive index of SiO_xN_y. The findings also suggest that to achieve the desirable optical properties of these films, silicon oxynitride must exhibit a high refractive index that lies between those of SiO_2 and Si_3N_4.

In conclusion, this paper provides valuable insight into the selection of experimental precursor deposition parameters based on the intended application.

ACKNOWLEDGMENT

The researchers express their gratitude to the University of Constantine 1 (Algeria) for conducting the ellipsometry analysis and to the LAAS of Toulouse for the LPCVD films depositions. The authors also thank Dr. Imen Aggoun for her valuable assistance with the English revision of this work.

CONFLICTS OF INTEREST

The authors declare that they have no conflicts of interest.

REFERENCES

[1] S. Nowa-Tatchun, C. Villeneuve-Faure, L. Boudou, and K. Makasheva, “Impact of silver nanoparticles embedded in a silica layer on the surface morphology of the structure: Evaluation by Atomic Force Microscopy”, in *Proc. of 2023 IEEE 23rd International Conference on Nanotechnology (NANO)*, 2023, pp. 233–236. DOI: 10.1109/NANO58406.2023.10231207.

[2] R. Radoi, C. Gherasim, and M. Dinescu, “Characterisation of laser ablated silicon oxynitride thin films”, *Journal of Alloys and Compounds*, vol. 286, nos. 1–2, pp. 309–312, 1999. DOI: 10.1016/S0925-8388(98)01026-3.

[3] P. Temple-Boyer, B. Hajji, J. L. Alay, J. R. Morante, and A. Martinez, “Properties of SiO_xN_y films deposited by LPCVD from $SiH_4/N_2O/NH_3$ gaseous mixture”, *Sensors and Actuators A: Physical*, vol. 78, nos. 1–3, pp. 52–55, 1999. DOI: 10.1016/S0924-4247(98)00344-6.

[4] S.-K. Cho, T.-Y. Cho, W. J. Lee, J. Ryu, and J. H. Lee, “Structural and gas barrier properties of hydrogenated silicon nitride thin films prepared by roll-to-roll microwave plasma-enhanced chemical vapor deposition”, *Vacuum*, vol. 188, art. 110167, 2021. DOI: 10.1016/j.vacuum.2021.110167.

[5] Y. N. Novikov, A. A. Gismatulin, I. P. Prosvirin, P. G. Bobovnikov, G. Ya. Krasnikov, and V. A. Gritsenko, “Short-range order and charge transport in silicon-rich pyrolytic silicon oxynitride”, *Journal of Non-Crystalline Solids*, vol. 599, art. 121984, 2023. DOI: 10.1016/j.jnoncrysol.2022.121984.

[6] T. Al Mousset *al.*, “Characterization of structural and dielectric properties of silicon nitride thin films deposited by PECVD”, in *Proc. of 2024 IEEE 5th International Conference on Dielectrics (ICD)*, 2024, pp.1–4. DOI: 10.1109/ICD59037.2024.10613222.

[7] A. Soman and A. Antony, “Broad range refractive index engineering of Si_xN_y and SiO_xN_y thin films and exploring their potential applications in crystalline silicon solar cells”, *Materials Chemistry and Physics*, vol. 197, pp. 181–191, 2017. DOI: 10.1016/j.matchemphys.2017.05.035.

[8] W.-J. Chen, Y.-C. Liu, Z.-Y. Wang, L. Gu, Y. Shen, and H.-P. Ma, “Physical and electrical properties of silicon nitride thin films with different nitrogen–oxygen ratios”, *Nanomaterials*, vol. 15, no. 13, p. 958, 2025. DOI: 10.3390/nano15130958.

[9] S. K. Sharma *et al.*, “PECVD based silicon oxynitride thin films for nano photonic on chip interconnects applications”, *Micron*, vol. 44, pp. 339–346, 2013. DOI: 10.1016/j.micron.2012.08.006.

[10] V. Kanclíř, J. Václavík, and K. Žídek, “Precision of silicon oxynitride refractive-index profile retrieval using optical characterization”, *Acta Physica Polonica A*, vol. 140, no. 3, pp. 215–221, 2021. DOI: 10.12693/APhysPolA.140.215.

[11] F. Mortreuil, L. Boudou, K. Makasheva, G. Teyssedre, and C. Villeneuve-Faure, “Influence of dielectric layer thickness on charge injection, accumulation and transport phenomena in thin silicon oxynitride layers: A nanoscale study”, *Nanotechnology*, vol. 32, art. 065706, 2020. DOI: 10.1088/1361-6528/abc38a.

[12] H. H. Canar, G. Bektaş, and R. Turan, “On the passivation performance of SiN_x, SiO_xN_y and their stack on c-Si wafers for solar cell applications: Correlation with optical, chemical and interface properties”, *Solar Energy Materials and Solar Cells*, vol. 256, art. 112356, 2023. DOI: 10.1016/j.solmat.2023.112356.

[13] A. Wolf *et al.*, "Revised parametrization of the recombination velocity at SiO_2/SiN_x-passivated phosphorus-diffused surfaces", *Solar Energy Materials and Solar Cells*, vol. 231, art. 111292, 2021. DOI: 10.1016/j.solmat.2021.111292.

[14] A. Evtukh *et al.*, "Structure and electrical conductivity of nanocomposite SiO_xN_y(Si) and $SiAl_zO_xN_y$(Si) films", *Journal of Alloys and Compounds*, vol. 690, art. 170879, 2023. DOI: 10.1016/j.jallcom.2023.170879.

[15] X. Jin, Y. Sun, L. Zhao, P. Li, and S. Ran, "Reactive spark plasma sintering of Si_2N_2O ceramic: Reaction process, microstructure, mechanical and dielectric properties", *Ceramics International*, vol. 50, no. 8, pp. 12802–12809, 2024. DOI: 10.1016/j.ceramint.2024.01.185.

[16] K. Makasheva, "New materials versus new design: Study on the physico-chemical and electrical properties of thin SiO_xN_y layers for their use in RF-MEMS switches", in *Proc. of 5e Colloque sur les Matériaux du Génie Electrique (MGE 2010)*, 2010, pp. 104–109.

[17] R. Mahamdi, L. Saci, F. Mansour, C. Molliet, P. Temple-Boyer, and E. Scheid, "Physico-chemical properties of SiO_xN_y thin films", *International Journal of Nano and Biomaterials*, vol. 2, nos. 1–5, pp. 347–353, 2009. DOI: 10.1504/IJNBM.2009.027731.

[18] R. Mahamdi *et al.*, "Ellipsometric and Rutherford Back scattering Spectrometry studies of SiO_xN_y films elaborated by plasma-enhanced chemical vapour deposition technique", *Journal of Nanoscience and Nanotechnology*, vol. 11, no. 10, pp. 9118–9122, 2011. DOI: 10.1166/jnn.2011.4303.

[19] C. Villeneuve-Faure *et al.*, "Kelvin force microscopy characterization of charging effect in thin a-SiO_xN_y:H layers deposited in pulsed plasma enhanced chemical vapor deposition process by tuning the Silicon-environment", *Journal of Applied Physics*, vol. 113, no. 20, art. 204102, 2013. DOI: 10.1063/1.4805026.

[20] M. Boulesbaa, "Spectroscopic ellipsometry and FTIR characterization of annealed SiO_xN_y: H films prepared by PECVD", *Optical Materials*, vol. 122, part B, art. 111693, 2021. DOI: 10.1016/j.optmat.2021.111693.

[21] H. L. Yang *et al.*, "Silicon oxynitride thin films by plasma-enhanced atomic layer deposition using a hydrogen-free metal-organic silicon precursor and N_2 plasma", *Materials Science in Semiconductor Processing*, vol. 164, art. 107607, 2023. DOI: 10.1016/j.mssp.2023.107607.

[22] I. Camps, A. Mariscal-Jimenez, and R. Serna, "Silicon oxynitride nanofilms prepared by PLD with controlled Eu-local concentration for broadband white light emitters", *Applied Surface Science*, vol. 613, art. 156037, 2023. DOI: 10.1016/j.apsusc.2022.156037.

[23] A. Beddiaf, "Etude et caracterisation optique de structures bicouches issues de la filiere: Nitrure de silicium", M.S. thesis, 2009. [Online]. Available: https://fac.umc.edu.dz/fstech/bib191.php?debut=96.

[24] H. G. Tompkins and E. A. Irene, *Handbook of Ellipsometry*. William Andrew, 2005, p. 857. DOI: https://doi.org/10.1007/3-540-27488-X.

[25] J. Rivory, "Characterization of inhomogeneous dielectric films by spectroscopic ellipsometry", *Thin Solid Films*, vols. 313–314, pp. 333–340, 1998. DOI: 10.1016/S0040-6090(97)00842-0.

[26] J. C. Maxwell Garnett, "Colours in metal glasses and in metalic films", *Proceedings of the Royal Society of London*, vol. 73, pp. 443–445, 1904. DOI: 10.1098/rspl.1904.0058.

[27] Z. Gong, R. Chen, H. Chen, and X. Lin, "Anomalous Maxwell-Garnett theory for photonic time crystals", *Applied Physics Reviews*, vol. 12, no. 3, art. 031414, 2025. DOI: 10.1063/5.0275246.

[28] E. D. Palik, *Handbook of Optical Constants of Solids*. Academic Press, San Diego, CA, 1998.